Doi: 10.31276/VJSTE.61(2).17-22

On the melting of interstitial alloys FeH, FeSi and FeC with a body-centred cubic structure under pressure

Nguyen Quang Hoc[1], Nguyen Thi Hoa[2], Tran Dinh Cuong[1*], Dang Quoc Thang[1]

[1]Hanoi National University of Education, Vietnam
[2]University of Transport and Communications, Hanoi, Vietnam

Received 18 October 2018; accepted 21 December 2018

Abstract:

Taking the model of interstitial alloy *AB* with a body-centred cubic structure and the condition of absolute stability for the crystalline state, we derive analytic expression for the temperature of the limit of absolute stability for the crystalline state, the melting temperature, and the equation for the melting curve of this alloy using the statistical moment method. The results allow us to determine the melting temperature of alloy *AB* under pressure as well as at zero pressure. In limit cases, we obtain the melting theory of main metal *A* with a body-centred cubic structure. The theoretical results are numerically applied for alloys FeH, FeSi and FeC using different potentials.

Keywords: **absolute stability of the crystalline state, interstitial alloy, statistical moment method.**

Classification number: **2.1**

Introduction

Alloys in general, and interstitial alloys in particular, are widely used in material technology and science. Therefore, they are of particular interest to many researchers.

The melting temperature (MT) of materials under pressure is a crucial problem in solid state physics and material science [1, 2]. The MT of crystal is usually is the Simon experimental equation:

$$\frac{P_m - P_0}{a} = (T_m - T_0)^c - 1 \tag{1.1}$$

where T_m is the MT, P_m is the melting pressure, a and c are constants, P_0 and T_0 are the pressure and the temperature, respectively, of the triple point on the phase diagram.

Normally, when the value of P_0 is small, we can write equation (1.1) in the form:

$$\frac{P_m}{a} = (T_m - T_0)^c - 1 \tag{1.2}$$

However, equation (1.2) cannot describe the melting of crystal at high pressures. Kumari, et al. [3] have introduced the following phenomenological equation:

$$\frac{\Delta T_m}{\left[T_0(P_m - P_0)\right]} = A + B\left(P_m - P_0\right) \tag{1.3}$$

where T_m and T_0 are the MT at pressures P_m and P_0, respectively, $\Delta T_m = T_m - T_0$, and A and B are constants. Equation (1.3) allows us to determine the MT of crystal at high pressures.

Theoretically, it is necessary to use the solid-liquid equilibrium to determine the MT of crystal. However, this does not allow us to explicitly express the MT. According to some researchers, the temperature corresponding to the absolute stability limit for crystalline state at a certain pressure (T_s) is close to the MT at the same pressure. Therefore, according to the authors of [4], the melting curve of crystal coincides with the curve representing the absolute stability limit for the crystalline state. Accordingly, the self-consistent phonon-field method and the one-particle distribution function are used to investigate the MT. However, the results are not consistent with experiments. This has led some scientists to conclude that the MT can

*Corresponding author: Email: trcuong1997@gmail.com.

never be found using the stability limit for the solid phase. Other researchers have used the correlation effect to calculate the temperature of the absolute stability limit for the crystalline state. Although the results of this are more exact, they are limited at low pressures.

In support of the statistical moment method (SMM), N. Tang and V.V. Hung [4, 5] show that we can, in fact, determine the MT using the solid phase of crystal. First, they determine the absolute stability temperature (T_s) at different pressures using the SMM and then carry out the regulation in order to find T_m from T_s. The results of the SMM correspond better with experiments than those of other methods.

The research content

Analytical results

In the model of the interstitial alloy *AB*, which has a body-centred cubic (BCC) structure, the large atoms *A* are in the peaks and the centre of the cube, and the smaller interstitial atoms *B* are in the centres of the cube faces. In [6-11], we derived the analytic expressions for the nearest neighbour distance, the cohesive energy and the alloy parameters for atoms *B, A,* and A_1 (the main atom *A* which is closest to atom *B*) and A_2 (the main atom *A* which is second closest to atom *B*).

The equations representing the state of the BCC interstitial alloy *AB* at temperature *T* and at zero temperature, respectively, are as follows:

$$Pv = -a_X\left[\frac{1}{6}\frac{\partial u_{0X}}{\partial a_X} + \theta x c t h x \frac{1}{2k_X}\frac{\partial k_X}{\partial a_X}\right] \quad (2.1)$$

$$Pv = -a_X\left[\frac{1}{6}\frac{\partial u_{0X}}{\partial a_X} + \frac{\hbar\omega_0}{4k_X}\frac{\partial k_X}{\partial a_X}\right] \quad (2.2)$$

From equation (2.2), we can calculate the nearest neighbour distance $a_x\ (P, 0)\ (X = B, A, A_1, A_2)$ and then the parameters $k_x\ (P, 0)$, $\gamma_{1x}\ (P, 0)$, $\gamma_{2x}\ (P, 0)$, and $\gamma_x\ (P, 0)$. The displacement of atoms from the equilibrium position is determined as in [6, 7]. From that, we can calculate the nearest neighbour distance $a_x\ (P, T)$ as follows:

$$a_B(P,T) = a_B(P,0) + y_{A_1}(P,T),\ a_A(P,T) = a_A(P,0) + y_A(P,T)$$
$$a_{A_1}(P,T) \approx a_B(P,T),\ a_{A_2}(P,T) = a_{A_2}(P,0) + y_B(P,T) \quad (2.3)$$

The approximate mean nearest neighbour distance between two atoms in the interstitial alloy *AB* is determined by:

$$a_{AB}(P,T) = a_{AB}(P,0) + y_{AB}(P,T)$$
$$a_{AB}(P,0) = (1-c_B)a_A(P,0) + c_B a'_A(P,0),\ a'_A(P,0) = \sqrt{3}a_B(P,0)$$
$$y_{AB}(P,T) = (1-7c_B)y_A(P,T) + c_B y_B(P,T) + 2c_B y_{A_1}(P,T) + 4c_B y_{A_2}(P,T) \quad (2.4)$$

The free energy of interstitial alloy *AB* with concentration condition $c_B << c_A$ has the form [6-11]:

$$\psi_{AB} = (1-7c_B)\psi_A + c_B\psi_B + 2c_B\psi_{A_1} + 4c_B\psi_{A_2} - TS_c$$
$$\psi_X \approx U_{0X} + \psi_{0X} + 3N\left\{\frac{\theta^2}{k_X^2}\left[\gamma_{2X}X_X^2 - \frac{2\gamma_{1X}}{3}\left(1+\frac{X_X}{2}\right)\right] + \right.$$
$$\left.\frac{2\theta^3}{k_X^4}\left[\frac{4}{3}\gamma_{2X}^2 X_X\left(1+\frac{X_X}{2}\right) - 2\left(\gamma_{1X}^2 + 2\gamma_{1X}\gamma_{2X}\right)\left(1+\frac{X_X}{2}\right)(1+X_X)\right]\right\}$$
$$U_{0X} = \frac{N}{2}u_{0X},\ \psi_{0X} = 3N\theta\left[x_X + \ln(1-e^{-2x_X})\right],\ X_X \equiv x_X \coth x_X \quad (2.5)$$

where ψ_A is the free ener.gy of atom *A* in the pure metal *A*, ψ_B is the free energy of atom *B* in the interstitial alloy *AB*, ψ_{A_1} and ψ_{A_2} are the free energy values of atoms A_1 and A_2, respectively, and S_c is the configuration entropy of the interstitial alloy *AB*.

The pressure is calculated as follows:

$$P = -\left(\frac{\partial\psi_{AB}}{\partial V_{AB}}\right)_T = -\frac{a_{AB}}{3V_{AB}}\left(\frac{\partial\psi}{\partial a_{AB}}\right)_T \quad (2.6)$$

Setting

$$\gamma_G^T = -\frac{a_{AB}}{6}\left[\frac{1}{k_A}\frac{\partial k_A}{\partial a_A}(1-7c_B)x_A\coth x_A + \frac{1}{k_B}\frac{\partial k_B}{\partial a_B}c_B x_B \coth x_B + \right.$$
$$\left.\frac{1}{k_{A_1}}\frac{\partial k_{A_1}}{\partial a_{A_1}}2c_B x_{A_1}\coth x_{A_1} + \frac{1}{k_{A_2}}\frac{\partial k_{A_2}}{\partial a_{A_2}}4c_B x_{A_2}\coth x_{A_2}\right] \quad (2.7)$$

where, γ_G^T is the Grüneisen parameter of alloy *AB*. Then,

$$P = -\frac{a_{AB}}{6V_{AB}}\left[(1-7c_B)\frac{\partial U_{0A}}{\partial a_A} + c_B\frac{\partial U_{0B}}{\partial a_B} + 2c_B\frac{\partial U_{0A_1}}{\partial a_{A_1}} + 4c_B\frac{\partial U_{0A_2}}{\partial a_{A_2}}\right] + \frac{3\gamma_G^T\theta}{V_{AB}} \quad (2.8)$$

From the condition of absolute stability limit

$$\left(\frac{\partial P}{\partial V_{AB}}\right)_T = 0 \quad \text{or} \quad \left(\frac{\partial}{\partial\ _{AB}}\right) \quad (2.9)$$

we can derive the absolute stability temperature for the crystalline state in the form:

$$T_s = \frac{TS_1}{MS_1},\ TS_1 = 2PV_{AB} + \frac{a_{AB}^2}{6}\left[(1-7c_B)\frac{\partial^2 U_{0A}}{\partial a_A^2} + c_B\frac{\partial^2 U_{0B}}{\partial a_B^2} + 2c_B\frac{\partial^2 U_{0A_1}}{\partial a_{A_1}^2} + 4c_B\frac{\partial^2 U_{0A_2}}{\partial a_{A_2}^2}\right] -$$

$$(1-7c_B)\left[\frac{a_{AB}}{2k_A}\left(\frac{\partial k_A}{\partial a_A}\right)^2-a_{AB}\frac{\partial^2 k_A}{\partial a_A^2}\right]\frac{\hbar\omega_A a_{AB}}{4k_A}-c_B\left[\frac{a_{AB}}{2k_B}\left(\frac{\partial k_B}{\partial a_B}\right)^2-a_{AB}\frac{\partial^2 k_B}{\partial a_B^2}\right]\frac{\hbar\omega_B a_{AB}}{4k_B}-$$

$$2c_B\left[\frac{a_{AB}}{2k_{A_1}}\left(\frac{\partial k_{A_1}}{\partial a_{A_1}}\right)^2-a_{AB}\frac{\partial^2 k_{A_1}}{\partial a_{A_1}^2}\right]\frac{\hbar\omega_{A_1} a_{AB}}{4k_{A_1}}-4c_B\left[\frac{a_{AB}}{2k_{A_2}}\left(\frac{\partial k_{A_2}}{\partial a_{A_2}}\right)^2-a_{AB}\frac{\partial^2 k_{A_2}}{\partial a_{A_2}^2}\right]\frac{\hbar\omega_{A_2} a_{AB}}{4k_{A_2}}$$

$$MS_1=(1-7c_B)\frac{a_{AB}^2k_{Bo}}{4k_A^2}\left(\frac{\partial k_A}{\partial a_A}\right)^2+c_B\frac{a_{AB}^2k_{Bo}}{4k_B^2}\left(\frac{\partial k_B}{\partial a_B}\right)^2+2c_B\frac{a_{AB}^2k_{Bo}}{4k_{A_1}^2}\left(\frac{\partial k_{A_1}}{\partial a_{A_1}}\right)^2+4c_B\frac{a_{AB}^2k_{Bo}}{4k_{A_2}^2}\left(\frac{\partial k_{A_2}}{\partial a_{A_2}}\right)^2 \quad (2.10)$$

In the case of zero pressure,

$$T_s=\frac{TS_2}{MS_2},TS_2=\frac{a_{AB}^2}{6}\left[(1-7c_B)\frac{\partial^2U_{0A}}{\partial a_A^2}+c_B\frac{\partial^2U_{0B}}{\partial a_B^2}+2c_B\frac{\partial^2U_{0A_1}}{\partial a_{A_1}^2}+4c_B\frac{\partial^2U_{0A_2}}{\partial a_{A_2}^2}\right]-$$

$$(1-7c_B)\left[\frac{a_{AB}}{2k_A}\left(\frac{\partial k_A}{\partial a_A}\right)^2-a_{AB}\frac{\partial^2 k_A}{\partial a_A^2}\right]\frac{\hbar\omega_A a_{AB}}{4k_A}-c_B\left[\frac{a_{AB}}{2k_B}\left(\frac{\partial k_B}{\partial a_B}\right)^2-a_{AB}\frac{\partial^2 k_B}{\partial a_B^2}\right]\frac{\hbar\omega_B a_{AB}}{4k_B}-$$

$$2c_B\left[\frac{a_{AB}}{2k_{A_1}}\left(\frac{\partial k_{A_1}}{\partial a_{A_1}}\right)^2-a_{AB}\frac{\partial^2 k_{A_1}}{\partial a_{A_1}^2}\right]\frac{\hbar\omega_{A_1} a_{AB}}{4k_{A_1}}-4c_B\left[\frac{a_{AB}}{2k_{A_2}}\left(\frac{\partial k_{A_2}}{\partial a_{A_2}}\right)^2-a_{AB}\frac{\partial^2 k_{A_2}}{\partial a_{A_2}^2}\right]\frac{\hbar\omega_{A_2} a_{AB}}{4k_{A_2}}$$

$$MS_2=(1-7c_B)\frac{a_{AB}^2k_{Bo}}{4k_A^2}\left(\frac{\partial k_A}{\partial a_A}\right)^2+c_B\frac{a_{AB}^2k_{Bo}}{4k_B^2}\left(\frac{\partial k_B}{\partial a_B}\right)^2+2c_B\frac{a_{AB}^2k_{Bo}}{4k_{A_1}^2}\left(\frac{\partial k_{A_1}}{\partial a_{A_1}}\right)^2+4c_B\frac{a_{AB}^2k_{Bo}}{4k_{A_2}^2}\left(\frac{\partial k_{A_2}}{\partial a_{A_2}}\right)^2 \quad (2.11)$$

Because the curve of the absolute stability limit for the crystalline state is close to the MS of crystal, the temperature (T_s) is usually high and $x_X\coth x_X\approx 1$ at T_s. Therefore,

$$\frac{1}{(1-7c_B)\frac{a_{AB}^2k_{Bo}}{4k_A^2}\left(\frac{\partial k_A}{\partial a_A}\right)^2+c_B\frac{a_{AB}^2k_{Bo}}{4k_B^2}\left(\frac{\partial k_B}{\partial a_B}\right)^2+2c_B\frac{a_{AB}^2k_{Bo}}{4k_{A_1}^2}\left(\frac{\partial k_{A_1}}{\partial a_{A_1}}\right)^2+4c_B\frac{a_{AB}^2k_{Bo}}{4k_{A_2}^2}\left(\frac{\partial k_{A_2}}{\partial a_{A_2}}\right)^2}\times$$

$$\left\{2PV_{AB}+\frac{a_{AB}^2}{6}\left[(1-7c_B)\frac{\partial^2U_{0A}}{\partial a_A^2}+c_B\frac{\partial^2U_{0B}}{\partial a_B^2}+2c_B\frac{\partial^2U_{0A_1}}{\partial a_{A_1}^2}+4c_B\frac{\partial^2U_{0A_2}}{\partial a_{A_2}^2}\right]-\right.$$

$$(1-7c_B)\left[\frac{a_{AB}}{2k_A}\left(\frac{\partial k_A}{\partial a_A}\right)^2-a_{AB}\frac{\partial^2 k_A}{\partial a_A^2}\right]\frac{\hbar\omega_A a_{AB}}{4k_A}-c_B\left[\frac{a_{AB}}{2k_B}\left(\frac{\partial k_B}{\partial a_B}\right)^2-a_{AB}\frac{\partial^2 k_B}{\partial a_B^2}\right]\frac{\hbar\omega_B a_{AB}}{4k_B}-$$

$$\left.2c_B\left[\frac{a_{AB}}{2k_{A_1}}\left(\frac{\partial k_{A_1}}{\partial a_{A_1}}\right)^2-a_{AB}\frac{\partial^2 k_{A_1}}{\partial a_{A_1}^2}\right]\frac{\hbar\omega_{A_1} a_{AB}}{4k_{A_1}}-4c_B\left[\frac{a_{AB}}{2k_{A_2}}\left(\frac{\partial k_{A_2}}{\partial a_{A_2}}\right)^2-a_{AB}\frac{\partial^2 k_{A_2}}{\partial a_{A_2}^2}\right]\frac{\hbar\omega_{A_2} a_{AB}}{4k_{A_2}}\right\}+$$

$$\frac{2V_{AB}}{k_{Bo}a_{AB}\left[\frac{1}{k_A}\frac{\partial k_A}{\partial a_A}(1-7c_B)+\frac{1}{k_B}\frac{\partial k_B}{\partial a_B}c_B+\frac{1}{k_{A_1}}\frac{\partial k_{A_1}}{\partial a_{A_1}}2c_B+\frac{1}{k_{A_2}}\frac{\partial k_{A_2}}{\partial a_{A_2}}4c_B\right]}\times$$

$$\left\{P+\frac{a_{AB}}{6V_{AB}}\left[(1-7c_B)\frac{\partial U_{0A}}{\partial a_A}+c_B\frac{\partial U_{0B}}{\partial a_B}+2c_B\frac{\partial U_{0A_1}}{\partial a_{A_1}}+4c_B\frac{\partial U_{0A_2}}{\partial a_{A_2}}\right]\right\}=0 \quad (2.12)$$

This is the equation for the curve of the absolute stability limit for the crystalline state. Therefore, the pressure is a function of the mean nearest neighbour distance:

$$P=P(a_{AB}) \quad (2.13)$$

Temperature $T_s(0)$ at zero pressure has the form:

$$T_s(0)=\frac{a_{AB}}{18\gamma_G^Tk_{Bo}}\left[(1-7c_B)\frac{\partial U_{0A}}{\partial a_A}+c_B\frac{\partial U_{0B}}{\partial a_B}+2c_B\frac{\partial U_{0A_1}}{\partial a_{A_1}}+4c_B\frac{\partial U_{0A_2}}{\partial a_{A_2}}\right] \quad (2.14)$$

where the parameters a_{AB}, $\frac{\partial U_{0X}}{\partial a_X}$, γ_G^T are determined at $T_s(0)$. Temperature T_s at pressure P has the form:

$$T_s\approx T_s(0)+\frac{V_{AB}P}{3k_{Bo}\left(\gamma_G^T\right)^2}\left(\frac{\partial\gamma_G^T}{\partial T}\right)_{a_{AB}}T_s \quad (2.15)$$

where k_{Bo} is the Boltzmann constant, $V_{AB},\gamma_G^T,\partial\gamma_G^T/\partial T$ are determined at T_s, and T_m is approximately the same as T_s. In order to solve equation (2.15), we can use the approximate iteration method. In the first approximate iteration,

$$T_{s1}\approx T_s(0)+\frac{V_{AB}(T_s(0))P}{3k_{Bo}\gamma_G(T_s(0))} \quad (2.16)$$

where $T_s(0)$ is the temperature of the absolute stability limit for the crystalline state at pressure P. Inserting T_{s1} into equation (2.15), we obtain a better approximate value (T_{s2}) for T_s at pressure P in the second approximate iteration:

$$T_{s2}\approx T_s(0)+\frac{V_{AB}(T_{s1})P}{3k_{Bo}\gamma_G(T_{s1})}-\frac{V_{AB}(T_{s1})P}{3k_{Bo}\gamma_G^2(T_{s1})}\left(\frac{\partial\gamma_G^T}{\partial T}\right)_{a_{AB}}T_{s1} \quad (2.17)$$

Analogously, we can obtain better approximate values for T_s at pressure P in the third, fourth, and subsequent approximate iterations. These approximations are applied at low pressures.

In the case of high pressure, the MT of the alloy at pressure P is calculated by:

$$T_m(P)=\frac{T_m(0)B_0^{\frac{1}{B_0'}}}{G(0)}.\frac{G(P)}{(B_0+B_0'P)^{\frac{1}{B_0'}}} \quad (2.18)$$

where $T_m(P)$ and $T_m(0)$ are the MT at pressure P and zero pressure, respectively, $G(P)$ and $G(0)$ are the shear modulus at pressure P and zero pressure, respectively,

B_0 is the isothermal elastic modulus at zero pressure, $B_0' = \left(\frac{dB_T}{dP}\right)_{P=0}$, and $B_T = B_T(P)$ is the isothermal elastic modulus at pressure P.

Numerical results for alloys FeH, FeSi and FeC

For alloys FeH, FeSi, and FeC, we use the Morse potential, the m - n potential, and the Finnis-Sinclair potential as follows:

$$\varphi(r) = D\left[e^{-2\alpha(r-r_0)} - 2e^{-\alpha(r-r_0)}\right] \quad (2.19)$$

$$\varphi(r) = \frac{D}{n-m}\left[m\left(\frac{r_0}{r}\right)^n - n\left(\frac{r_0}{r}\right)^m\right] \quad (2.20)$$

$$U = -A\sqrt{\sum_{i\neq j}\rho(r_{ij})} + \frac{1}{2}\sum_{i\neq j}\varphi(r_{ij})$$

$$\rho(r) = t_1(r-R_1)^2 + t_2(r-R_1)^3 \quad (r<R_1)$$
$$\varphi(r) = (r-R_2)^2(k_1 + k_2 r + k_3 r^2) \quad (r<R_2) \quad (2.21)$$

The Morse potential parameters for Fe-Fe and Fe-H are shown in Table 1, the m - n potential parameters for Fe-Si are presented in Table 2, and the Finnis-Sinclair potential parameters for Fe-C are shown in Table 3.

Table 1. The Morse potential parameters for Fe-Fe [12] **and Fe-H** [13].

Interaction	D(eV)	α (Å)$^{-1}$	r_0(Å)
Fe-Fe	0.42	1.40	2.85
Fe-H	0.32	1.34	1.73

Table 2. The m - n potential parameters for Fe-Si [14].

Interaction	m	n	D(eV)	r_0(Å)
Fe-Si	2.0	5.5	1.06	2.3845

Table 3. The Finnis-Sinclair potential parameters for Fe-C [15].

A (eV)	R_1 (Å)	t_1 (Å)$^{-2}$	t_2 (Å)$^{-3}$	R_2 (Å)	k_1 (eV(Å)$^{-2}$)	k_2 (eV(Å)$^{-3}$)	k_3 (eV(Å)$^{-4}$)
2.958787	2.545937	10.024001	1.638980	2.468801	8.972488	-4.086410	1.483233

Our numerical results for the MT of alloys FeH, FeSi and FeC are summarized in Tables 4-7 and described in Figs. 1-6.

Table 4. The MT (T_m) of metal Fe under pressure obtained from the SMM and the experimental data (EXPT) [16].

P (GPa)	1	2	3	4	5	6
T_m - SMM	1861.43	1911.07	1959.08	2005.61	2050.77	2094.69
T_m - EXPT	1873	1908	1943	1978	2013	2033

Note that the MT of Fe at P = 0 is taken from EXPT [17], the MT of FeH at P = 0 is taken from EXPT [18], and the MT of FeSi and FeC at P = 0 are taken from EXPT [19].

Table 5. The MT (T_m) of alloy FeH under pressure obtained from the SMM.

c_H (%)	P (GPa)	1	2	3	4	5	6	8	10
0		1861.43	1911.07	1959.08	2005.61	2050.77	2094.69	2179.09	2259.44
1		1858.50	1905.28	1950.51	1994.31	2036.80	2078.08	2157.38	2232.78
2		1855.41	1899.17	1941.47	1982.40	2022.09	2060.64	2134.61	2204.87
3	T_m (K)	1852.16	1892.77	1932.00	1969.95	2006.73	2042.42	2110.87	2175.82
4		1848.77	1886.11	1922.15	1957.00	1990.76	2023.50	2086.24	2145.70
5		1845.26	1879.20	1911.94	1943.59	1974.23	2003.93	2060.77	2114.58

Table 6. The MT (T_m) of alloy FeSi under pressure obtained from the SMM.

c_{Si} (%)	P (GPa)	1	2	3	4	5	6	8	10
0		1861.43	1911.07	1959.08	2005.61	2050.77	2094.69	2179.09	2259.44
1		1838.56	1884.48	1928.86	1971.84	2013.54	2054.06	2131.86	2205.84
2		1821.81	1864.13	1905.00	1944.56	1982.90	2020.13	2091.57	2159.41
3	T_m (K)	1805.02	1843.68	1881.01	1917.10	1952.07	1985.99	2051.02	2112.68
4		1788.18	1823.16	1856.90	1889.50	1921.06	1951.66	2010.23	2065.69
5		1771.30	1802.56	1832.68	1861.77	1889.89	1917.14	1969.22	2018.45

Table 7. The MT (T_m) of alloy FeC under pressure obtained from the SMM.

c_C (%)	P (GPa)	1	2	3	4	5	6	8	10
0		1861.43	1911.07	1959.08	2005.61	2050.77	2094.69	2179.09	2259.44
1		1801.22	1845.45	1888.22	1929.66	1969.88	2008.96	2084.05	2155.50
2		1755.24	1794.55	1832.56	1869.38	1905.12	1939.84	2006.55	2069.98
3	T_m (K)	1709.51	1744.12	1777.60	1810.03	1841.51	1872.09	1930.84	1986.69
4		1664.07	1694.29	1723.53	1751.85	1779.34	1806.04	1857.32	1906.07
5		1618.98	1645.12	1670.40	1694.91	1718.68	1741.78	1786.14	1828.29

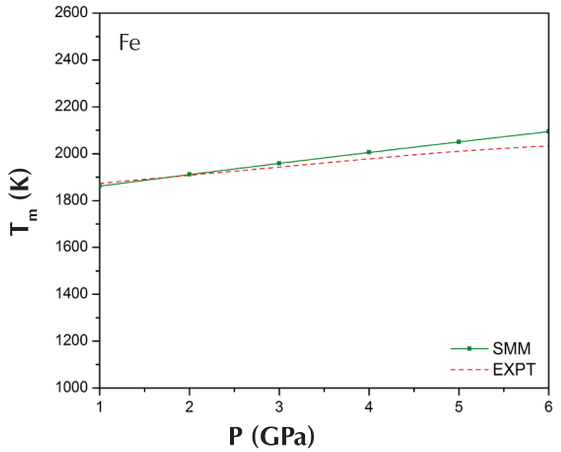

Fig. 1. $T_m(P)$ of Fe obtained from the SMM and EXPT [16].

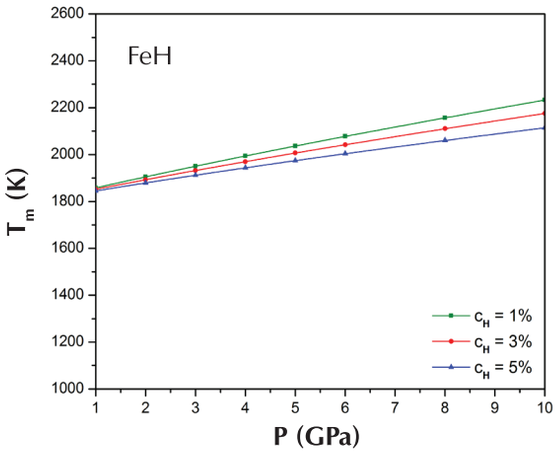

Fig. 2. $T_m(P)$ of FeH obtained from the SMM.

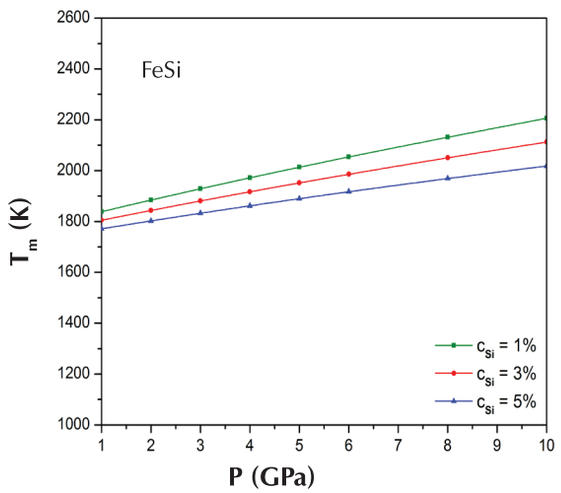

Fig. 3. $T_m(P)$ of FeSi obtained from the SMM.

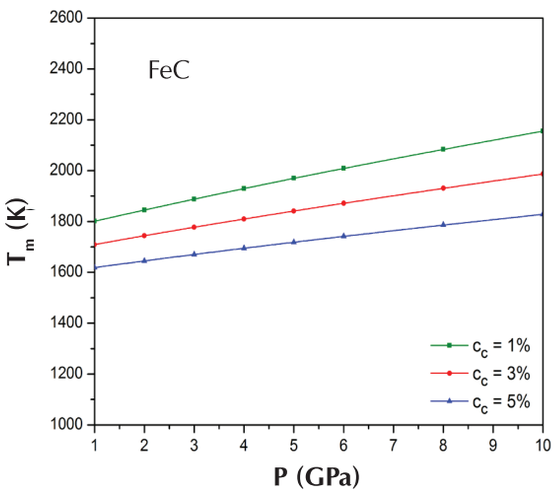

Fig. 4. $T_m(P)$ of FeC obtained from the SMM.

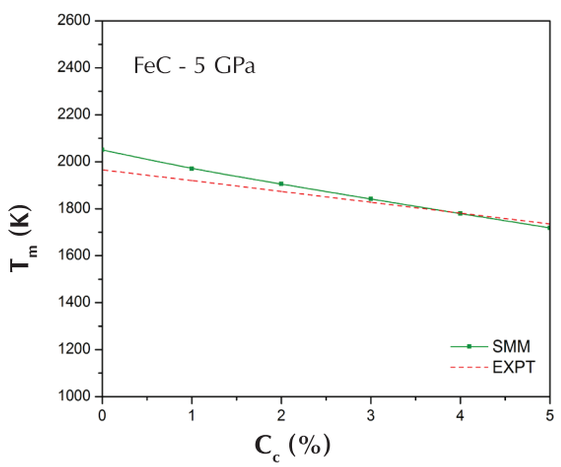

Fig. 5. $T_m(c_C)$ of FeC at 5 GPa obtained from the SMM and EXPT [20].

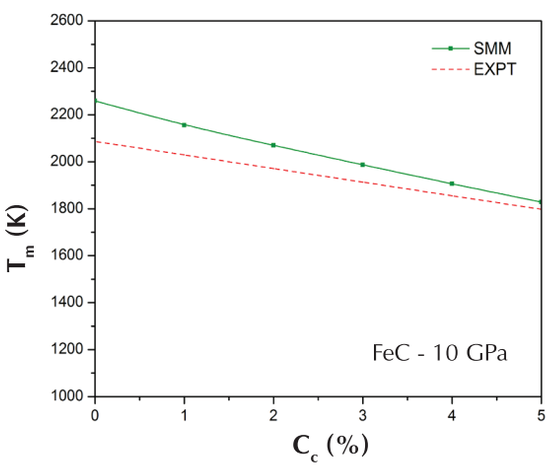

Fig. 6. $T_m(c_C)$ of FeC at 10 GPa obtained from the SMM and EXPT [20].

For the pure metal Fe, the SMM's results correspond well with experiments [16]. In the range of pressure from 0 to 6 GPa, the differences are lower than 3%. When pressure increases, the MT of Fe also increases.

For the interstitial alloys FeH, FeSi, and FeC with the same concentration of interstitial atoms, the MT also increases when pressure increases. For example, at $c_B = 5\%$, when the pressure (P) increases from 1 to 10 GPa, the MT (T_m) of FeH increases from 1845.26 to 2114.58 K, the MT (T_m) of FeSi increases from 1771.30 to 2018.45 K, and the MT (T_m) of FeC increases from 1618.98 to 1828.29 K.

At the same pressure, the MTs of alloys FeH, FeSi and FeC decrease when the concentration of interstitial atoms increases. For example, at P = 10 GPa when the concentration (c_B) increases from 0 to 5%, the MT (T_m) of FeH decreases from 2259.44 to 2114.58 K, the MT (T_m) of FeSi decreases from 2259.44 to 2018.45 K, and the MT (T_m) of FeC decreases from 2259.44 to 1828.29 K. When their the physical conditions are the same, the MT of FeC is lower than that of FeSi, the MT of FeSi is lower than that of FeH, and the MTs of the interstitial alloys FeH, FeSi and FeC are lower than the MT of Fe.

Figures 5 and 6 show that the MT (T_m) of FeC from the SMM corresponds well with EXPT [20]. The differences are lower than 4.3% at P = 5 GPa and lower than 8.3% at P = 10 GPa.

Conclusions

Using the SMM, we derive the analytic expressions for the temperature of the limit of absolute stability for the crystalline state, the MT, and the melting curve of the binary interstitial alloy at different pressures and concentrations of interstitial atoms. In limit cases, we obtain the melting theory of main metal A with a BCC structure. The theoretical results are numerically applied for alloys FeH, FeSi and FeC using the Morse potential, the m - n potential, and the Finnis-Sinclair potential.

The authors declare that there is no conflict of interest regarding the publication of this article.

REFERENCES

[1] A.B. Belonoshko, S.I. Simak, A.E. Kochetov, B. Johansson, L. Burakovsky and D.L. Preston (2004), "High-pressure melting of molybdenum", *Phys. Rev. Lett.,* **92(19)**, p.195701.

[2] L. Burakovsky, et al. (2000), "Analysis of dislocation mechanism for melting of elements: pressure dependence", *Journal of Applied Physics*, **88(11)**, p.6294.

[3] M. Kumari, K. Kumari, and N. Dass (1987), "On the melting law at high pressure", *Phys. Stat. Sol. (a)*, **99(1)**, pp.K23-K26.

[4] N. Tang and V.V. Hung (1998), "Investigation of the thermodynamic properties of anharmonic crystals by the momentum method. I. General results for face-centred cubic crystals", *Phys. Stat. Sol. (b),* **149(2)**, pp.511-519.

[5] V.V. Hung, K. Masuda-Jindo (2000), "Application of statistical moment method to thermodynamic properties of metals at high pressures", *J. Phys. Soc. Jpn.*, **69**, pp.2067-2075.

[6] N.Q. Hoc, D.Q. Vinh, B.D. Tinh, N.L. Phuong, T.T.C. Loan, T.T. Hue, D.T.T. Thuy (2015), "Thermodynamic properties of binary interstitial alloys with BCC structure: dependence on temperature and concentration of interstitial atoms", *HNUE Journal of Science: Mathematical and Physical Sciences*, **60(7)**, pp.146-155.

[7] N.Q. Hoc, D.Q. Vinh, N.T. Hang, N.T. Nguyet, L.X. Phuong, N.N. Hoa, N.T. Phuc, and T.T. Hien (2016), "Thermodynamic properties of a ternary interstitial alloy with BCC structure: dependence on temperature, concentration of substitution atoms and concentration of interstitial atoms", *HNUE Journal of Science: Mathematical and Physical Sciences*, **61(7)**, pp.65-74.

[8] N.Q. Hoc and N.D. Hien (2017), "Study on elastic deformation of interstitial alloy AB with BCC structure under pressure", *Proceedings of the 10th National Conference on Solid State Physics and Material Science* (*SPMS*), pp.911-914.

[9] N.Q. Hoc, N.T. Hoa, D.Q. Vinh (2017), "Study on the melting temperature of substitution alloy AB with interstitial atom C and BCC structure under pressure", *Journal of Science of Hanoi Pedagogical University No.2*, **50**, pp.130-143.

[10] N.Q. Hoc and N.D. Hien (2018), "Study on elastic deformation of substitution alloy AB with interstitrial atom C and BCC structure under pressure", *Journal of Physics: Conf. Series,* **1034(1)**, 012005.

[11] N.Q. Hoc, B.D. Tinh, D.Q. Vinh (2018), "Study on the melting of interstitial alloy AB with FCC structure under pressure", *Physics and Astronomy International Journal*, **2(3)**, pp.231-235.

[12] N.V. Hung, T.T. Hue, N.B. Duc (2015), "Calculation of morse potential parameters of bcc crystals and applications to anharmonic interatomic effective potentias, local force constant", *VNU Journal of Science: Mathematics - Physics*, **31(3)**, pp.23-30.

[13] J. Bardeen and C. Herring (1951), *Atom movements*, Ed. J.H. Hollomon, p.260.

[14] M.N. Magomedov (1987), "Calculation of the debye temperature and the gruneisen-parameter", *J. Fiz. Khimic*, **61(4)**, pp.1003-1009.

[15] T.L. Timothy, J.F. Clemens, Xi Lin, D.G. Julian, Y. Sidney, J.V.V. Krystyn (2007), "Many-body potential for point defect clusters in Fe-C alloys", *Phys. Rev. Lett.*, **98(21)**, 215501.

[16] A.F. Guillermet & P. Gustafson (1984), "An assessment of the thermodynamic properties and the (p, T) phase diagram of iron", *High Temp.-High Press.*, **16(6)**, pp.591-610.

[17] E. Yu Tonkov, E.G. Ponyatovsky (2005), *Phase transformations of elements under high pressure*, CRC Press.

[18] A. San-Martin, F.D. Manchester (1990), "The Fe-H (iron-hydrogen) system", *Bulletin of Alloy Phase Diagrams*, **11(2)**, pp.173-184.

[19] H. Okamoto (2000), *Desk handbook: phase diagrams for binary alloys*, ASM International.

[20] O.T. Lord, M.J. Walter, R. Dasgupta, D. Walker, S.M. Clark (2009), "Melting in the Fe–C system to 70 GPa", *Earth and Planetary Science Letters*, **284(1-2)**, pp.157-167.